RSC Advances

PAPER

View Article Online
View Journal | View Issue

Cite this: *RSC Adv.*, 2025, **15**, 32299

Mn(II) betadiketonates: structural diversity from deceptively minor alterations to synthetic protocols

Mukaila A. Ibrahim, [a] René T. Boeré *[b] and Kathryn E. Preuss *[a]

Received 22nd May 2025
Accepted 20th August 2025

DOI: 10.1039/d5ra03587b

rsc.li/rsc-advances

In the context of the importance of manganese β-diketonates as precursors for the preparation of manganese oxide thin films and nanostructured materials, we report synthetic protocols and pitfalls encountered in the preparation of a family of Mn(II) complexes of two fluorinated β-diketonates, 1,1,1-trifluoroacetylacetonato- (tfac) and 1,1,1,5,5,5-hexafluoroacetylacetonato- (hfac). The synthetic conditions and crystal structures of six new complexes are reported, including a coordination polymer $\{K[Mn(tfac)_3]\}_\infty$, an unusual trinuclear complex $Mn_3(tfac)_6(OH_2)_2$, and a series of mononuclear complexes with coordinated solvents tetrahydrofuran, 1,2-dimethoxyethane, water, and acetonitrile. The crystal structures of two known Mn(II) complexes are also reported for completeness.

Introduction

Fluorinated β-diketonate complexes of Mn(II) and Mn(III) are versatile starting materials for the development of Mn_xF_y and Mn_xO_y thin films and nanostructured materials.[1,2] Manganese oxides are particularly attractive owing to their low toxicity, elemental abundance, variety of stoichiometries and morphologies, and potential applications.[3–5] The mixed valent Mn_3O_4 oxide is one stoichiometry of interest, with a range of possible applications, including supercapacitor electrodes,[6] catalysts,[7–9] gas sensors,[10] and magnetic media.[11] As another example, the MnO_2 stoichiometry adopts a range of morphologies that are attracting attention in the field of energy storage, specifically for application as supercapacitors in the design of flexible devices.[12,13] Recent studies demonstrate synthetic control over Mn_xF_y and Mn_xO_y thin film stoichiometry and morphology using β-diketonate precursors for chemical vapour deposition (CVD) fabrication.[1,2] Evidently, promising technological applications of Mn_xO_y materials, and the possibility of low-cost CVD or atomic layer deposition (ALD) fabrication, make fluorinated β-diketonate complexes of manganese worthy of further investigation. Nevertheless, the structural and synthetic diversity of Mn(II) β-diketonate complexes reported in the current literature remains surprisingly limited.

The main goal of this work is to establish reproducible synthetic protocols for anhydrous divalent Mn(II) complexes of the 1,1,1-trifluoroacetylacetonato- (tfac) and 1,1,1,5,5,5-hexafluoroacetylacetonato- (hfac) β-diketonates with labile solvent ligands, tetrahydrofuran (THF) and 1,2-dimethoxyethane (DME). These complexes can then be used as synthetic precursors to Mn(II) β-diketonate complexes of more exotic ligands, either for CVD and ALD applications or for other purposes. For example, we have found anhydrous $Mn(hfac)_2(THF)_2$ (ref. 14 and 15) to be valuable for the synthesis of $Mn(hfac)_2(L)$ complexes, where L is an air-sensitive paramagnetic ligand.[15–19] Our particular interest in exploring the use of $Mn(hfac)_2(DME)$ and the analogous $Mn(tfac)_2(DME)$ complex as alternate precursors stems from a desire to manipulate the stability and reactivity of these precursors for use in solution-based and mechanochemical syntheses. Additionally, we are interested in the role of the fluorinated β-diketonates in controlling volatility and solubility, crystal lattice structure and softness, and metal ion hardness/softness and redox behaviour, especially in coordination complexes of paramagnetic ligands. As our synthetic trials toward the desired Mn(II) β-diketonate precursors progressed, we uncovered anhydrous and aqua intermediates with interesting structural diversity. Our findings are reported herein and serve, in part, as a cautionary tale regarding reproducibility and the effects of relatively minor modifications to synthetic strategies.

Results and discussion

Although tfac and hfac are structurally very similar, differing only by one group (CH_3 *vs.* CF_3 at one site), the account we present herein demonstrates marked differences in chemical behaviour and coordination product architectures. Rationale for these differences is not immediately obvious and is likely related to a combination of factors. In general, β-diketonate ligands are weak-field ligands, as are all the solvent ligands used

[a]*Department of Chemistry, University of Guelph, Guelph, ON N1G 2W1, Canada. E-mail: kpreuss@uoguelph.ca*

[b]*Department of Chemistry and Biochemistry and The Canadian Centre for Advanced Fluorine Technologies, University of Lethbridge, Lethbridge, AB T1K 3M4, Canada. E-mail: boere@uleth.ca*

in this study, thus it is reasonable to expect Mn(II) to be high-spin in all cases. As a hs-d^5 metal ion, hs-Mn(II) exhibits zero ligand field stabilization enthalpy such that the coordination geometry is mechanically flexible and the position of coordinated ligands about the metal centre is primarily dependent on steric factors, including the optimization of crystal packing in the solid state. In the context of hard–soft-acid–base theory, hfac is expected to be a harder base than tfac and therefore has higher affinity for a hard metal acid. While Mn(II) is a hard acid, there is evidence that it tolerates softer bases better than other hard acid metal ions.[20] Furthermore, the hardness of the Mn(II) ion is altered by the coordination of one or more β-diketonate ligands. For example, Mn(II) is harder when coordinated to the more electron-withdrawing hfac than when coordinated to tfac, affecting its coordination behaviour with other ligands such as solvent ligands and a second or third β-diketonate ligand. As β-diketonate ligands are weak Lewis bases, pH also plays a role when protic species are present. Finally, the relative solubility of equilibria products using tfac *vs.* hfac is also a relevant factor, owing to differences in polarity (hfac being more polar) and dispersion interactions (weaker dispersion forces are expected for the more highly fluorinated hfac).

To understand the context in which each of the species reported herein has been observed, it is necessary to start by

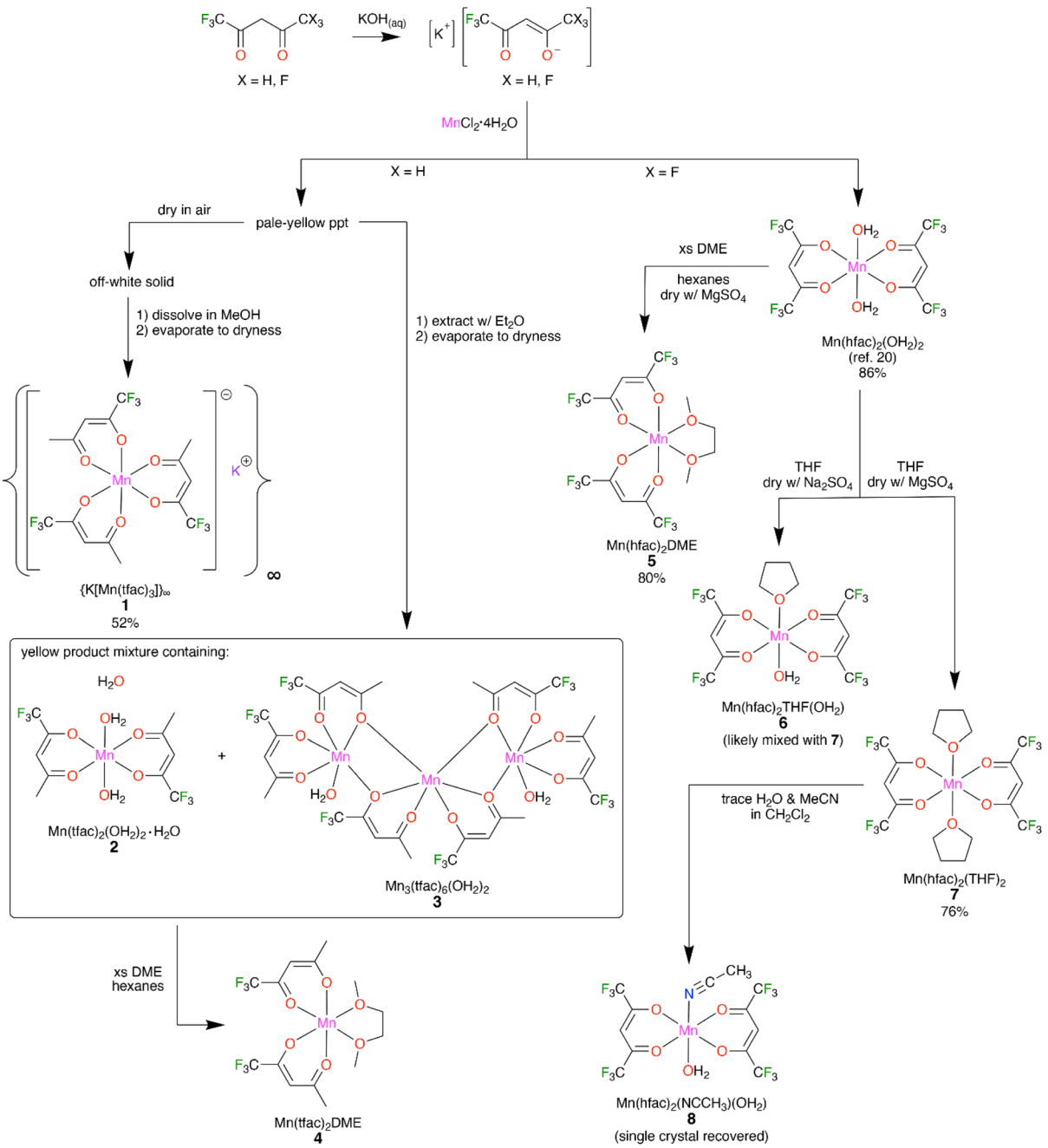

Scheme 1 Reaction scheme showing relationship between complexes **1**–**8**, and including known complex $Mn(hfac)_2(OH_2)_2$.

describing the reactions and observations (Scheme 1). The first step of the synthetic protocol is essentially the same for all complexes. The protonated β-diketonate, either Htfac or Hhfac, is deprotonated using a stoichiometric amount of KOH in water to generate the anion, tfac or hfac, nominally as a potassium salt. A stoichiometric amount of $MnCl_2 \cdot 4H_2O$ is then added and the resulting yellow precipitate is recovered. When the β-diketone employed is 1,1,1,5,5,5-hexafluoroacetylacetone (Hhfac), the recovered material is the diaqua complex, $Mn(hfac)_2(OH_2)$, which has been previously reported[21] and confirmed herein by IR.

However, when 1,1,1-trifluoroacetylacetone (Htfac) is used, the results are strikingly different. The initial pale-yellow precipitate, when dried in air, becomes an off-white solid. Single crystal X-ray diffractometry (SCXRD) of crystals grown by dissolution of the off-white solid in MeOH and subsequent evaporation of the solvent reveals a polymeric structure $\{K[Mn(tfac)_3]\}_\infty$ of alternating K^+ cations and $[Mn(tfac)_3]^-$ anions (**1**, Fig. 1, Table 1). The IR spectrum of this off-white solid confirms the absence of a ν(O–H) stretch and thus the absence of water. The combustion elemental analysis of the bulk recrystallized material is consistent with the $\{K[Mn(tfac)_3]\}_\infty$ structure.

The polymeric $\{K[Mn(tfac)_3]\}_\infty$ may be a viable precursor to the target DME and THF complexes, but it is an inefficient intermediate as it is not representative of the stoichiometric 2-to-1 ratio of β-diketonate to Mn(II) employed in the synthesis, nor of the desired ratio in the subsequent target complexes. Recalling that this off-white polymeric solid was recovered from drying a pale-yellow material that was initially recovered from the reaction mixture, we took a different approach. Once the initial pale-yellow precipitate had formed, diethyl ether was

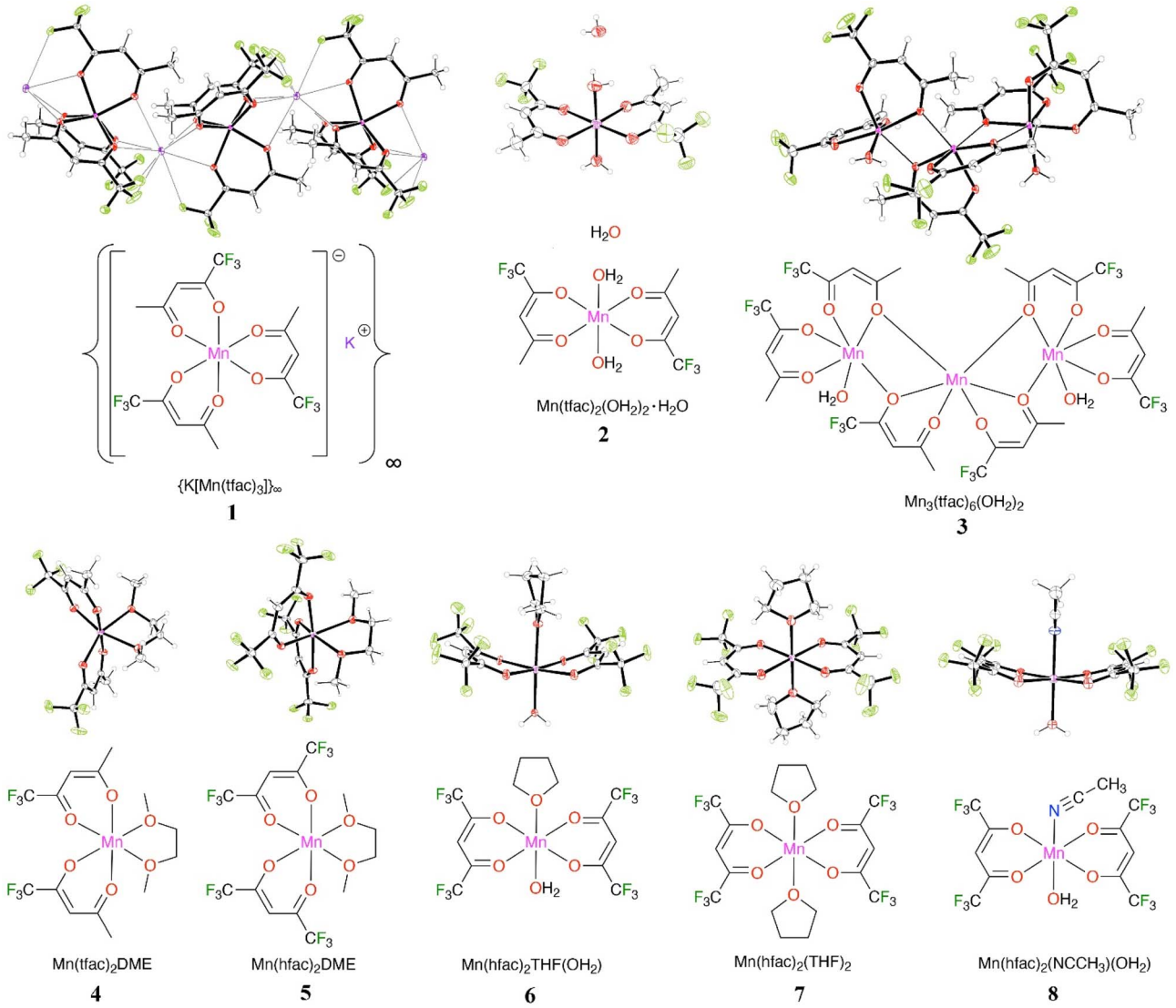

Fig. 1 Excerpts of the crystal structures of complexes **1**–**8** depicted as ORTEP representations with thermal ellipsoids drawn in a range of 10–35% for visual clarity; colour code: Mn, magenta; O, red; F, green; K, purple; N, blue; C, grey; H, white spheres. For effects of site symmetry and the (omitted) minor disorder components, see Experimental.

Table 1 Summary of select structural attributes of complexes **1–8**

Complex	β-Diketonate ligand	Solvent ligand	Coordination geometry (coordination number = 6)	Shortest/longest Mn–O bond (Å)	Smallest/largest O–Mn–O angle (°)	Space group
$\{K[Mn(tfac)_3]\}_\infty$ **1**	tfac	—	Trigonal prismatic	2.158(2)/2.1742(15)	79.59(9)/138.19(5)	*Pnma*
$Mn(tfac)_2(OH_2)_2 \cdot H_2O$ **2**	tfac	H_2O	Octahedral, *trans*-	2.137(5)/2.175(5)	83.47(17)/178.04(17)	$P2_1/c$
$Mn_3(tfac)_6(OH_2)_2$ **3**	tfac	H_2O	Octahedral, *cis*-	2.1048(16)/2.2944(15)	75.26(5)/171.86(6)	$P\bar{1}$
$Mn(tfac)_2(DME)$ **4**	tfac	DME	Distorted octahedral, *cis*-	2.1000(14)/2.3127(14)	72.86(5)/178.76(6)	*Pbca*
$Mn(hfac)_2(DME)$ **5**	hfac	DME	Distorted octahedral, *cis*-	2.1092(15)/2.2246(17)	74.00(6)/170.93(7)	$P2_1/c$
$Mn(hfac)_2(OH_2)(THF)$ **6**	hfac	H_2O, THF	Octahedral, *trans*-	2.130(5)/2.229(4)	84.92(17)/174.04(19)	$C2/c$
$Mn(hfac)_2(THF)_2$ **7**	hfac	THF	Octahedral, *trans*-	2.1450(11)/2.2057(16)	83.94(4)/179.27(7)	*Pnma*
$Mn(hfac)_2(OH_2)(NCCH_3)$ **8**	hfac	H_2O, CH_3CN	Octahedral, *trans*-	2.139(4)/2.155(7) Mn–N 2.283(8)	84.08(16)/175.90(17)	*Pnma*

added to the reaction mixture, dissolving the solids. The ether layer was separated from the aqueous layer, which was washed with additional ether to recover any remaining product, and yellow crystalline material was recovered from slow evaporation of the combined organic layers. While the IR spectrum indicated the presence of an aqua ν(O–H) stretch suggesting the product might be analogous to that obtained when hfac is the β-diketonate, combustion analysis (found: C, 27.96; H, 3.48%) did not match the calculated elemental ratio for $Mn(tfac)_2(OH_2)_2$; calculated for $MnC_{10}H_{12}O_6F_6$: C, 30.24; H, 3.05%. Structural analysis of a single crystal selected from the bulk material revealed an interesting trinuclear complex $Mn_3(tfac)_6(OH_2)_2$ (**3**, Fig. 1). However, the calculated elemental ratio for this trimer does not match the results from the combustion analysis either; calculated for $Mn_3C_{30}H_{28}F_{18}O_{14}$: C, 32.19; H, 2.52%. In a separate but identical synthesis, a single crystal recovered from the bulk yellow crystalline material proved to be the mononuclear bis(aqua) complex with a co-crystallized water, $Mn(tfac)_2(OH_2)_2 \cdot H_2O$ (**2**, Fig. 1). The calculated elemental ratio (calculated for $MnC_{10}H_{14}O_7F_6$: C, 28.93; H, 3.4%) is closer to the results of the combustion analysis, but still inadequate to definitively identify the bulk solid. In all cases, the IR spectrum of the bulk material was essentially identical. It is likely that the bulk material is a mixture of complexes, possibly dominated by the mononuclear bis(aqua) species co-crystallized with water, $Mn(tfac)_2(OH_2)_2 \cdot H_2O$ (**2**, Fig. 1). Nevertheless, the bulk material was readily converted to the DME complex, $Mn(tfac)_2(DME)$ (**4**, Fig. 1), by stirring a suspension in hexanes with the addition of excess DME. For comparison, the analogous $Mn(hfac)_2(DME)$ complex (**5**, Fig. 1) is prepared in a similar manner, by stirring the $Mn(hfac)_2(OH_2)_2$ complex[21] in hexanes with the addition of excess DME.

Although stoichiometric synthetic protocols appear to reliably yield the anticipated mononuclear products when hfac is the β-diketonate employed, we observed an interesting result in one specific instance when attempting to prepare the THF adduct, $Mn(hfac)_2(THF)_2$ (**7**, Fig. 1). A typical preparation of $Mn(hfac)_2(THF)_2$ involves the dissolution of $Mn(hfac)_2(OH_2)_2$ in dry THF under inert atmosphere, with either Na_2SO_4 or $MgSO_4$ added as a drying agent. In this instance, Na_2SO_4 was used and the result was a complex in which only one of the two aqua ligands had been replaced by THF, $Mn(hfac)_2(OH_2)(THF)$ (**6**, Fig. 1). Indeed, it is well-documented that $MgSO_4$ is a superior drying agent to Na_2SO_4 in water-miscible solvents such as acetonitrile,[22,23] and Na_2SO_4 is generally not recommended for drying ethers. Use of Na_2SO_4 requires more time, and even with an extended period, drying may not go to completion. However, concern regarding the possible scrambling of Mg^{2+} with Mn^{2+} owing to anomalously low lability of Mg^{2+},[24,25] and the subsequent difficulty in separating structurally similar Mg(II) and Mn(II) complexes, can make Na_2SO_4 an alternative worth considering. Interestingly, in this work a first structure determination of **5**, using precipitated rather than sublimed crystals, displays unusually low electron density, corresponding to a refined 'apparent occupancy' of only 0.90, for the metal. This could have been caused by partial replacement of Mn^{2+} with Mg^{2+} in the crystal (see Section 6 in the SI for details). A better structure on sublimed crystals has largely resolved the anomaly for **5**, but this remains a concern in Mn(II) chemistry. We have also included the conditions for a successful preparation of $Mn(hfac)_2(THF)_2$ (**7**) for completeness.

As detailed above, we have observed the incomplete displacement of aqua ligands with THF when using $Mn(hfac)_2(OH_2)_2$ as the starting material. In fact, we have also observed the reverse scenario. In a failed attempt to displace the THF ligands of $Mn(hfac)_2(THF)_2$ with a custom-designed *N*,*N*′-bidentate ligand, we recovered thin yellow needles of $Mn(hfac)_2(OH_2)(THF)$ (**6**, Fig. 1) as well as deep yellow block crystals of $Mn(hfac)_2(OH_2)(NCCH_3)$ (**8**, Fig. 1). A mixture of these two crystalline solids was isolated as a precipitate from a dichloromethane solution at −18 °C. The acetonitrile was introduced inadvertently, likely with the custom-designed ligand that had been recrystallized from acetonitrile. It is interesting that both species recovered in this instance were mono-aqua with another donor solvent ligand.

The coordination polymer $\{K[Mn(tfac)_3]\}_\infty$ crystallizes in the orthorhombic space group *Pnma* and consists of alternating K^+ cations and $[Mn(tfac)_3]^-$ anions (**1**; Fig. 1–3) forming a 1D zigzag structure propagating in [100]. There is one Mn atom and one K atom per asymmetric unit, and the $K[Mn(tfac)_3]$ monomeric unit is bisected by a mirror plane that relates two of the tfac ligands by reflection. The arrangement of bidentate tfac ligands around the Mn(II) in the anionic $[Mn(tfac)_3]^-$ complex forms a roughly trigonal prismatic coordination geometry, however

the tfac ligands are oriented such that only two of the three –CF_3 groups extend in the same direction along the chain. This arrangement of tfac ligands allows for the intercalation of the K^+ cations between two $[Mn(tfac)_3]^-$ anions, with close contacts to six O atoms; specifically, to one O atom of each tfac ligand on each of the two flanking $[Mn(tfac)_3]^-$ complexes. Additionally, there are close contacts between K^+ and tfac F atoms; specifically, there are two short contacts to F atoms from one $[Mn(tfac)_3]^-$ complex, and only one such F contact from the anion complex on the other side. The resulting 9-coordinate environment about K^+ has K···O distances ranging from 2.7440(15) to 3.054(2) Å and K···F distances of 3.078(2) and 3.114(2) Å.

A similar coordination polymer, with hfac ligands *in lieu* of tfac ligands, $\{K[Mn(hfac)_3]\}_\infty$ has been reported previously,[26] but with striking differences in crystal packing (Fig. 2). Unlike $\{K[Mn(tfac)_3]\}_\infty$, in which zigzag-shaped 1D structures propagating along [100] are aligned parallel to one another, $\{K[Mn(hfac)_3]\}_\infty$ crystallizes in the cubic space group $Pa\bar{3}$ (no. 205), with linear-shaped 1D structures propagating in three different directions, generating the 3-fold symmetry of the space group. Furthermore, the hfac ligands provide three additional contacts to the intercalated K^+ ions, generating a 12-coordinate environment with K···O and K···F distances similar to those found in $\{K[Mn(tfac)_3]\}_\infty$ (K···O distances: 2.746(3) to 2.822(3) Å; K···F distances: 3.110(3) to 3.153(3) Å). Indeed, it is the difference in coordination environment of the K^+ in these two polymers that generates the zigzag 1D structure in one and the linear 1D structure in the other (Fig. 3).

Similar coordination polymers, with alternating metal monocations and $[M(hfac)_3]^-$ anions, are also known for other metal ions, including $\{Na[Mn(hfac)_3]\}_\infty$,[27] $\{In[Mn(hfac)_3]\}_\infty$,[14] $\{K[Co(hfac)_3]\}_\infty$,[28] and $\{K[Ni(hfac)_3]\}_\infty$.[29] However, a search of the Cambridge Structural Database reveals only one previously reported example of such a coordination polymer in which tfac is the β-diketonate, $\{Na[Ni(tfac)_3]\}_\infty$.[30] As the Na^+ ion is smaller than the K^+ ion, the Na···O distances tend to be shorter and the Na···F contacts are outside the range normally considered to be coordinating (Na···O distances: 2.351(7) to 2.447(7) Å; Na···F distances: 3.151(7) to 3.223(7) Å). Thus, the Na^+ ions are best described as being 6-coordinate in both $\{Na[Mn(hfac)_3]\}_\infty$ and $\{Na[Ni(tfac)_3]\}_\infty$. The smaller ionic radius and resulting lower coordination number of Na^+ compared to K^+ also means that the nature of the β-diketonate plays a lesser role in the structure of the coordination polymers in which Na^+ is the intercalated counterion. For example, the zigzag shape of the 1D structure in $\{K[Mn(tfac)_3]\}_\infty$ is reinforced by short K···F contacts, whereas the $\{Na[Ni(tfac)_3]\}_\infty$ polymer, with longer Na···F contacts, has a nearly linear arrangement of the Na^+ and Ni^{2+} ions along the polymer backbone (Fig. 2 and 3).

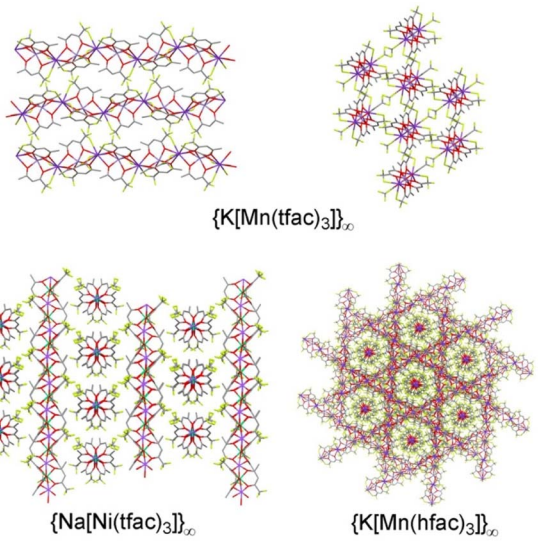

Fig. 2 Top: Excerpts of the crystal structure of coordination polymer **1** $\{K[Mn(tfac)_3]\}_\infty$ showing the crystal packing of 1D structures from two different perspectives. Bottom: Excerpts of the crystal structures of $\{Na[Ni(tfac)_3]\}_\infty$ (CSD refcode: DOKBIQ)[30] and $\{K[Mn(hfac)_3]\}_\infty$ (CSD refcode: LILHET)[26] showing the crystal packing of analogous 1D coordination polymers discussed in the text.

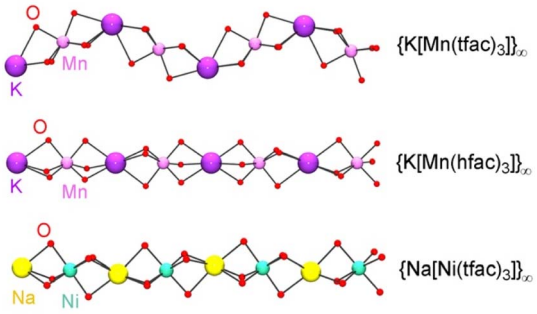

Fig. 3 Excerpts of the crystal structures of polymer **1** $\{K[Mn(tfac)_3]\}_\infty$, $\{K[Mn(hfac)_3]\}_\infty$ (CSD refcode: LILHET)[26] and $\{Na[Ni(tfac)_3]\}_\infty$ (CSD refcode: DOKBIQ)[30] showing only the metal ions and oxygen atoms to illustrate the zigzag *vs.* linear 1D structures; colour code: Mn, pink; K, purple; Ni, turquoise; Na, yellow; O, red.

In the unsuccessful quest to isolate a mononuclear $Mn(tfac)_2(OH_2)_2$ aqua complex, the $\{K[Mn(tfac)_3]\}_\infty$ polymer **1** was one of three species isolated and identified. The other species were the water solvate of the target complex, $Mn(tfac)_2(OH_2)_2 \cdot H_2O$ **2**, and an unusual trinuclear complex $Mn_3(tfac)_6(OH_2)_2$ **3**, which can be described as a linear trimer of $Mn(tfac)_2$ units with a coordinated aqua ligand at each end (Fig. 1). Trimer **3** appears to represent a unique structure type. An extensive search of the Cambridge Structural Database reveals no known analogous structures, either with tfac or hfac as the β-diketonate, or with other metal ions. Crystallizing as discrete trimeric molecules in $P\bar{1}$, with $Z' = 1$, complex **3** includes three symmetry inequivalent Mn nuclei supported by reciprocal short Mn···O contacts (ranging from 2.221(1) to 2.294(2) Å) between neighbouring $Mn(tfac)_2$ units. Each Mn^{2+} centre is 6-coordinate with an approximately octahedral coordination geometry. Indeed, the range of contact distances between $Mn(tfac)_2$ units overlaps with the range of the Mn–O bond distances of the chelating tfac ligands (ranging from 2.105(2) to 2.251(1) Å). Thus, the structure is best described by invoking bridging O atoms of the tfac ligands and considering the short Mn···O contacts as Mn–O bonds.

While the coordination geometry about the Mn^{2+} ions in polymer **1** is approximately trigonal prismatic, an approximately octahedral coordination geometry is observed in both the mononuclear species **2** and the trinuclear species **3**. The monodentate aqua ligands in **2** are *trans*- to one another, whereas in **3** the monodentate coordination sites are *cis*- to one another (Fig. 1). This diversity in coordination geometry reflects the absence of ligand field stabilization enthalpy associated with a 6-coordinate hs-d^5 transition metal ion; both aqua and β-diketonates are weak-field ligands. Furthermore, the isolation of three different crystalline materials under similar synthetic conditions suggests an equilibrium in solution that allows for displacement of negatively charged tfac ligands. Indeed, similar equilibria products have been observed for acetylacetonato- (acac) complexes of Mn(II) *via in situ* monitoring of the formation of $Mn(acac)(OH_2)_2$, where it was noted that pH is a contributing factor.[31] Aqua complexes of hs-Mn^{2+} are typically considered to be labile with water exchange-rate constants at ambient temperature measured or calculated to be on the order of 10^7 to 10^9 s^{-1} (Langford–Gray Class II).[25,32,33] The important conclusion drawn from these observations is that care should be exercised to correctly characterize products when repeating seemingly straight-forward synthetic protocols for Mn^{2+} coordination complexes, even for bidentate anionic ligands such as tfac.

Comparing the structures of mononuclear complexes **2** and **4–8** (Fig. 1), we see several factors influencing the coordination geometry. Those species incorporating monodentate ligands (complexes **2**, **6**, **7**, and **8**) all adopt a roughly octahedral coordination geometry with the monodentate ligands *trans*- to one another. The structure of **7** has previously been reported (CSD refcode: NOBWIL).[14] The implication is that this geometry reduces crowding and steric strain from the relatively bulky β-diketonate ligands. It is worth noting that the aqua ligands in the related $Mn(hfac)_2(OH_2)_2$ structure are reported to be *cis*- to one another,[26,34] supporting 1D supramolecular structures defined by reciprocal H-bonding between the coordinated aqua H atoms and the hfac O atoms (Fig. 4). By contrast both the hydrate $Mn(tfac)_2(OH_2)_2\cdot H_2O$ **2** and the previously reported hfac analogue with co-crystallized water, $Mn(hfac)_2(OH_2)_2\cdot H_2O$,[35] adopt a geometry in which the coordinated aqua ligands are *trans*- to one another. While the former crystallizes in $P2_1/c$ and the latter in *Pnma*, both exhibit H-bonding between the co-crystallized water molecules, coordinated aqua ligands, and β-diketonate ligands (Fig. 4). It can be inferred that stabilization gained from the network of H-bonds is sufficient to offset any steric strain resulting from the *cis*-conformation in the unsolvated $Mn(hfac)_2(OH_2)_2$ crystal structure, but that incorporation of co-crystallized water molecules allows for favourable packing of the *trans*-conformer. Indeed, other known co-crystals of $Mn(hfac)_2(OH_2)_2$ show both *cis*- and *trans*-conformations, with an apparent dependence on H-bonding as a contributing factor.[36–39]

Furthermore, observations regarding the conformations of Mn(II) β-diketonates with monodentate ligands suggest that complexes **4** and **5**, in which the β-diketonate ligands are necessarily *cis*- to one another owing to bidentate coordination

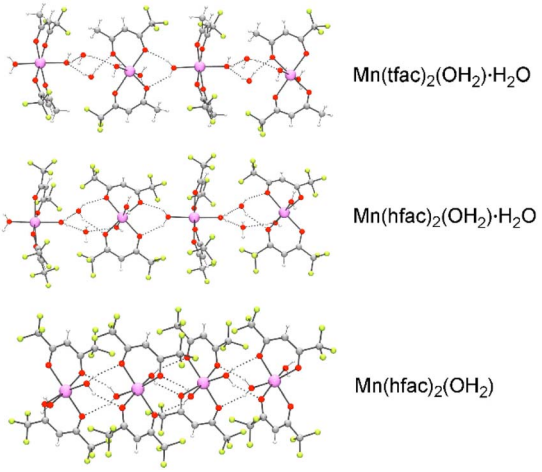

Fig. 4 Excerpts from the crystal structures of $Mn(tfac)_2(OH_2)_2\cdot H_2O$ **2**, $Mn(hfac)_2(OH_2)_2\cdot H_2O$ (CSD refcode: TUDFON),[35] and $Mn(hfac)_2(OH_2)_2$ (CSD refcode: LIKZOU)[26] highlighting H-bonding; colour code: Mn, pink; O, red; F, green; C, grey; H, white.

of DME, may be more highly strained despite the absence of effects from ligand field stabilization enthalpy. Both the $Mn(tfac)_2$DME complex **4** and the $Mn(hfac)_2$DME complex **5** adopt distorted octahedral coordination geometries, although **4** appears somewhat more distorted, possibly owing to differences in deformation as a result of the crystal packing. These DME coordination complexes may be preferable to those with monodentate ligands for our purpose of employing them as anhydrous precursors for coordination to air-sensitive chelating ligands. The rationale being that the structures are pre-organized to the desired *cis*- conformation, which may facilitate formation of the target complexes.

Experimental

General considerations

All purchased reagents were used as received. 1,1,1,5,5,5-Hexafluoroacetylacetone (Hhfac) and manganese(II) chloride tetrahydrate ($MnCl_2\cdot 4H_2O$) were purchased from Strem Chemicals Inc. 1,1,1-Trifluoroacetylacetone (Htfac) and DME were purchased from Sigma-Aldrich. Hexanes, THF, potassium hydroxide (KOH), sodium sulfate (Na_2SO_4), and magnesium sulfate ($MgSO_4$) were purchased from Fisher. Deionized (DI) water was provided through a building-wide plumbed system. THF was dried over sodium benzophenone ketyl and distilled prior to use. Infrared (IR) spectra were recorded on a Thermo Fisher Scientific Nicolet iS50 FTIR spectrometer at ambient temperature and 4 cm^{-1} resolution; samples were prepared as Nujol mulls on KBr plates; peaks are categorized with acronyms vs = very strong, s = strong, m = moderate, w = weak. Copies of IR spectra of pure phases are provided in Section 10 of the SI. Melting points were determined visually on a Mel-Temp melting point apparatus. Elemental analyses were performed at Brock University.

Preparation of potassium tris(1,1,1-trifluoroacetylacetonato) manganate(II) polymer $\{K[Mn(tfac)_3]\}_\infty$ 1. Htfac (2.0 mL, 16.5

mmol) was added to a solution of KOH (0.925 g, 16.5 mmol) in 80 mL DI water. After 20 min. stirring, $MnCl_2 \cdot 4H_2O$ (1.63 g, 8.24 mmol) was added and the mixture was stirred for 2 h. The resulting pale-yellow precipitate was recovered by suction filtration and dried in air to afford an off-white solid with a yield of 1.52 g (2.75 mmol based on repeat unit m. w. = 553.29 g mol^{-1}; 50.2%); m. p. > 260 °C. Crystals of $\{K[Mn(tfac)_3]\}_\infty$ **1** suitable for SCXRD were grown from methanol by slow evaporation to dryness. FTIR (Nujol, cm^{-1}): 1625s, 1529m, 1501m, 1459s, 1376m, 1298m, 1227m, 1189m, 1135m, 855w, 769w, 728w, 568w. Elemental analysis calculated for $KMnC_{15}H_{12}F_9O_6$: C, 32.56; H, 2.19%. Found: C, 32.56; H, 1.99%.

Crystal data for **1** ($C_{15}H_{12}F_9KMnO_6$, M =553.29 g mol^{-1}): orthorhombic, space group *Pnma* (no. 62), $a = 13.4514(3)$ Å, $b = 13.7819(3)$ Å, $c = 10.8398(2)$ Å, $V = 2009.55(7)$ Å^3, $Z = 4$, $T = 100.01(10)$ K, μ(Cu Kα) = 8.293 mm^{-1}, $D_{calc} = 1.829$ g cm^{-3}, 10 677 reflections measured ($10.382° \leq 2\Theta \leq 160.454°$), 2268 unique ($R_{int} = 0.0440$, $R_{sigma} = 0.0316$) which were used in all calculations. The final R_1 was 0.0378 ($I > 2\sigma(I)$) and wR_2 was 0.1032 (all data). CCDC 2441294.

Preparation of dimethoxyethanebis(1,1,1-trifluoroacetylacetonato)manganese(II) Mn(tfac)$_2$(DME) 4. Htfac (2.9 mL, 24.0 mmol) was added to a solution of KOH (1.39 g, 24.0 mmol) in 150 mL DI water. After 20 min. stirring, $MnCl_2 \cdot 4H_2O$ (2.37 g, 12.0 mmol) was added and the mixture was stirred for a further 20 min. producing a pale-yellow precipitate. Diethyl ether (50 mL) was added, dissolving the solids. The ether layer was recovered and the aqueous layer was washed with a further 50 mL ether. The combined organic layers were washed with a concentrated aqueous solution of KI. The ether was removed by slow evaporation in the air to afford a yellow solid; yield 3.155 g; m. p. 158–160 °C. FTIR (Nujol, cm^{-1}): 3400s, br ν(O–H), 3315m, 3285m, 1675m, 1635s, 1528s, 1289vs, 1231m, 1194s, 1135vs, 1025w, 1012w, 944w, 857m, 783m, 757w, 728m, 610w, 571m, 517w, 417w. Single crystals suitable for SCXRD were recovered from the bulk yellow solid and determined to be the mononuclear aqua complex with co-crystallized water $Mn(tfac)_2(OH_2)_2 \cdot H_2O$ **2** and the trinuclear complex $Mn_3(tfac)_6(OH_2)_2$ **3**. Combustion analysis demonstrated that neither the mononuclear complex **2**, nor the trimer **3**, nor the target $Mn(tfac)_2(OH_2)_2$ complex, are representative of the bulk material. Elemental analysis calculated for $MnC_{10}H_{12}O_6F_6$: C, 30.24; H, 3.05%. Calculated for $MnC_{10}H_{14}O_7F_6$: C, 28.93; H, 3.4%. Calculated for $Mn_3C_{30}H_{28}F_{18}O_{14}$: C, 32.19; H, 2.52%. Found: C, 27.96; H, 3.48%. Nevertheless, the yellow product mixture was successfully converted to Mn(tfac)$_2$(DME) **4**. Excess DME (3 mL) was added to a suspension of unidentified bulk yellow material (2.50 g) in 100 mL hexanes and this mixture was stirred for 2 h to afford a greenish-yellow solution. Water was removed from the reaction mixture using $MgSO_4$. The drying agent was removed by gravity filtration using Whatman Grade 5 filter paper. The solution was concentrated to 10 mL *in vacuo* and placed in the freezer (−18 °C). Greenish-yellow block crystals of Mn(tfac)$_2$(DME) **4** grew overnight. These were recovered by filtration and dried under vacuum; yield 2.32 g (5.54 mmol); m. p. 78–80 °C. FTIR (Nujol, cm^{-1}): 3298w, 3141w, 1648vs, 1601s, 1560s, 1533s, 1256vs, 1207s, 1148vs, 1095s, 1060s, 1026s, 1010s, 950m, 865s, 833m, 800s, 767m, 741m, 722m, 666s, 585s, 527w, 482w. Elemental analyses calculated for $MnC_{14}H_{18}F_6O_6$: C, 37.27; H, 4.02%. Found: C, 37.03; H, 3.90%.

Crystal data for **2** ($C_{10}H_{14}O_7F_6Mn$, M =415.15 g mol^{-1}): monoclinic, space group $P2_1/c$ (no. 14), $a = 10.9445(8)$ Å, $b = 6.9902(5)$ Å, $c = 21.9193(19)$ Å, $\beta = 102.495(8)°$, $V = 1637.2(2)$ Å^3, $Z = 4$, $T = 100.00(10)$ K, μ(Cu Kα) = 7.482 mm^{-1}, D_{calc} = 1.684 g cm^{-3}, 13 112 reflections measured ($8.264° \leq 2\Theta \leq 135.49°$), 2937 unique ($R_{int} = 0.1096$, $R_{sigma} = 0.0685$) which were used in all calculations. The final R_1 was 0.0891 ($I > 2\sigma(I)$) and wR_2 was 0.2524 (all data). CCDC 2441295.

Crystal data for **3** ($C_{30}H_{28}F_{18}Mn_3O_{14}$, M =1119.34 g mol^{-1}): triclinic, space group $P\bar{1}$ (no. 2), $a = 10.7690(2)$ Å, $b = 11.5144(3)$ Å, $c = 16.9696(4)$ Å, $\alpha = 85.497(2)°$, $\beta = 76.820(2)°$, $\gamma = 84.015(2)°$, $V = 2034.35(8)$ Å^3, $Z = 2$, $T = 100.01(10)$ K, μ(Cu Kα) = 8.822 mm^{-1}, D_{calc} = 1.827 g cm^{-3}, 44 915 reflections measured ($5.358° \leq 2\Theta \leq 160.618°$), 8821 unique ($R_{int} = 0.0320$, $R_{sigma} = 0.0252$) which were used in all calculations. The final R_1 was 0.0339 ($I > 2\sigma(I)$) and wR_2 was 0.0940 (all data). CCDC 2441296.

Crystal data for **4** ($C_{14}H_{18}F_6MnO_6$, M =451.22 g mol^{-1}): orthorhombic, space group *Pbca* (no. 61), $a = 12.4430(6)$ Å, $b = 13.5342(6)$ Å, $c = 21.9592(12)$ Å, $V = 3698.1(3)$ Å^3, $Z = 8$, $T = 150.15$ K, μ(MoKα) = 0.800 mm^{-1}, D_{calc} = 1.621 g cm^{-3}, 38 776 reflections measured ($3.71° \leq 2\Theta \leq 50.49°$), 3345 unique ($R_{int} = 0.0564$, $R_{sigma} = 0.0312$) which were used in all calculations. The final R_1 was 0.0295 ($I > 2\sigma(I)$) and wR_2 was 0.0660 (all data). CCDC 2441638.

Preparation of diaquabis(1,1,1,5,5,5-hexafluoroacetylacetonato)manganese(II) Mn(hfac)$_2$(OH$_2$)$_2$. Mn(hfac)$_2$(OH$_2$)$_2$ was prepared using modifications to a literature method.[21] Hhfac (2.0 mL, 14.1 mmol) was added to a solution of KOH (0.793 g, 14.1 mmol) in 80 mL DI water. After 20 min. stirring, $MnCl_2 \cdot 4H_2O$ (1.39 g, 7.05 mmol) was added and the mixture was stirred for 2 h. The resulting yellow precipitate was recovered by suction filtration and dried in air to afford a yellow solid with a yield of 3.07 g (6.08 mmol; 86.2%). The IR spectrum matches the literature with the water ν(O–H) stretch of 3448 cm^{-1}.[21]

Preparation of dimethoxyethanebis(1,1,1,5,5,5-hexafluoroacetylacetonato)manganese(II) Mn(hfac)$_2$(DME) 5. Excess DME (3 mL) was added to a suspension of Mn(hfac)$_2$(OH$_2$)$_2$ (2.41 g, 4.77 mmol) in 100 mL hexanes and the mixture was stirred for 2 h to afford a yellow solution. Water was removed from the reaction mixture using $MgSO_4$. The drying agent was removed by gravity filtration using Whatman Grade 5 filter paper, with the filtrate collected in a side-arm flask under argon flow. The solvent of the filtrate was removed *in vacuo* to afford a yellow crystalline solid. Mn(hfac)$_2$(DME) **5** was purified by sublimation in a three-zone furnace under vacuum (10^{-2} mbar) at 55 °C to give yellow block crystals suitable for SCXRD; yield 2.285 g (4.08 mmol; 85.6%); m. p. 74–76 °C. FTIR (Nujol, cm^{-1}): 3258w, 1624vs, 1523m, 1286vs, 1218w, 1182m, 1132vs, 1096w, 1053w, 1015w, 977w, 940w, 855w, 818w, 784w, 773w, 727w, 610w, 569w, 517w, 474w, 449w. Elemental analysis calculated for $MnC_{14}H_{12}F_{12}O_6$: C, 30.07; H, 2.16%. Found: C, 30.39; H, 2.77%.

Crystal data for **5** ($C_{14}H_{12}F_{12}MnO_6$, M =559.18 g mol^{-1}): monoclinic, space group $P2_1/n$ (no. 14), a = 11.9426(3) Å, b = 12.8936(3) Å, c = 14.0015(3) Å, β = 100.799(2)°, V = 2117.81(9) Å^3, Z = 4, T = 100.00(15) K, μ(Cu Kα) = 6.359 mm^{-1}, D_{calc} = 1.754 g cm^{-3}, 20 736 reflections measured (8.944° ≤ 2Θ ≤ 150.016°), 4248 unique (R_{int} = 0.0348, R_{sigma} = 0.0251) which were used in all calculations. The final R_1 was 0.0391 ($I > 2\sigma(I)$) and wR_2 was 0.1056 (all data). CCDC 2441639.

Preparation of bis(tetrahydrofuran)bis(1,1,1,5,5,5-hexafluoroacetylacetonato)manganese(II) Mn(hfac)$_2$(THF)$_2$ 7. Mn(hfac)$_2$(OH$_2$)$_2$ (1.00 g, 1.98 mmol) was dissolved in 40 mL dry THF under argon in a 250 mL side-arm flask and stirred at room temperature for 2 h to afford a yellow solution. Water was removed from the reaction mixture using $MgSO_4$. The drying agent was filtered with a filter stick. The solution was concentrated to 10 mL *in vacuo* and placed in the freezer (−18 °C). Orangish-yellow block crystals grew overnight, recovered by filtration, and dried *in vacuo*, yielding 0.92 g (76%). The crystal selected for SCXRD analysis was determined to be the Mn(hfac)$_2$(THF)$_2$ **7**. FTIR (Nujol, cm^{-1}): 3295w, 3149w, 1733w, 1715w, 1646s, 1606w, 1561m, 1536m, 1501s, 1351m, 1259vs, 1205s, 1150vs, 1095s, 1033s, 947w, 922w, 872m, 803s, 741w, 722w, 665s, 585m.

In an identical reaction attempt using Na_2SO_4 as the drying agent, *in lieu* of $MgSO_4$, a yellow crystalline solid was recovered by filtration, and dried *in vacuo*; yield: 0.87 g. The FTIR spectrum clearly identified the presence of water, but also suggested a mixture of materials from incomplete conversion to the target complex **7**. The yellow solid was sublimed on a programmable temperature tube furnace (55–70 °C) under dynamic vacuum (10^{-2} torr) yielding yellow block crystals. The crystal selected for SCXRD analysis was determined to be Mn(hfac)$_2$(OH$_2$)(THF) **6**. FTIR of the sublimation product (Nujol, cm^{-1}): 3463w ν(O–H), 3291w, 3142w, 1648vs, 1561s, 1538s, 1349m, 1259vs, 1205vs, 1147vs, 1092s, 1020w, 949w, 918m, 870w, 810s, 772w, 744w, 722w, 666s, 546s, 528w, 485w, 451w.

Thin yellow needles of Mn(hfac)$_2$(OH$_2$)(THF) **6** and deep yellow block crystals of Mn(hfac)$_2$(OH$_2$)(NCCH$_3$) **8** were also recovered from an unsuccessful attempt to displace both THF ligands of Mn(hfac)$_2$(THF)$_2$ **7** with a custom-designed *N*,*N*′-bidentate ligand, wherein H_2O and trace CH_3CN were inadvertently introduced to a CH_2Cl_2 solution.

Crystal data for **6** ($C_{14}H_{12}F_{12}MnO_6$, M =559.18 g mol^{-1}): monoclinic, space group $C2/c$ (no. 15), a = 21.5361(3) Å, b = 6.81320(10) Å, c = 27.8521(5) Å, β = 104.621(2)°, V = 3954.39(11) Å^3, Z = 8, T = 99.99(10) K, μ(Cu Kα) = 6.811 mm^{-1}, D_{calc} = 1.878 g cm^{-3}, 40 093 reflections measured (6.56° ≤ 2Θ ≤ 160.85°), 4294 unique (R_{int} = 0.0672, R_{sigma} = 0.0304) which were used in all calculations. The final R_1 was 0.0941 ($I > 2\sigma(I)$) and wR_2 was 0.2417 (all data). CCDC 2441297.

Crystal data for **7** ($C_{18}H_{18}O_6F_{12}Mn$, M =613.26 g mol^{-1}): orthorhombic, space group *Pnma* (no. 62), a = 15.4825(8) Å, b = 19.6279(8) Å, c = 7.7219(4) Å, V = 2346.6(2) Å^3, Z = 4, T = 150.03 K, μ(MoKα) = 0.691 mm^{-1}, D_{calc} = 1.736 g cm^{-3}, 40 469 reflections measured (4.15° ≤ 2Θ ≤ 54.932°), 2764 unique (R_{int} = 0.0278, R_{sigma} = 0.0128) which were used in all calculations. The final R_1 was 0.0308 ($I > 2\sigma(I)$) and wR_2 was 0.0812 (all data). CCDC 2441640. Improves on a previous 173 K structure determination (CSD refcode: NOBWIL).[14]

Crystal data for **8** ($C_{12}H_7NO_5F_{12}Mn$, M =528.13 g mol^{-1}): orthorhombic, space group *Pnma* (no. 62), a = 9.1029(3) Å, b = 21.7344(6) Å, c = 9.0051(3) Å, V = 1781.62(10) Å^3, Z = 4, T = 100.0(2) K, μ(Cu Kα) = 7.488 mm^{-1}, D_{calc} = 1.969 g cm^{-3}, 7617 reflections measured (8.136° ≤ 2Θ ≤ 149.832°), 1770 unique (R_{int} = 0.0406, R_{sigma} = 0.0239) which were used in all calculations. The final R_1 was 0.0766 ($I > 2\sigma(I)$) and wR_2 was 0.1821 (all data). CCDC 2441298.

Crystallography

Crystal and refinement parameters for all structures are compared in a summary table in the SI. Full details of the SCXRD data collection and structure model determinations are available in the remainder of the SI or from the archival CIF file, including tables of interatomic distances, angles, torsions and H-bonding parameters, to which interested readers are directed. Here, we list some additional complexities of the structure models and refinements that are either omitted or not immediately obvious from Fig. 1.

In structure **1**, the coordination polymer lies on a crystallographic mirror plane such that the Mn and K ions, as well as one of the tfac ligands are in special positions. The methyl H-atoms of C10 are therefore 50 : 50 disordered by reflection symmetry.

In the structure of **2**, there is an extensive network of H-bonds involving the coordinated aqua ligands and co-crystallized water, as well as three of the four tfac O atoms as acceptors. The parameters are listed in Section 3, Table S15 of the SI.

The novel trimeric cluster in structure **3** comprises the asymmetric unit of the crystal, which are linked only by two distinct H-bonds of the aqua ligands to neighbours in the lattice. See Section 4, Table S23 of the SI for these parameters. The C5, C9, C19 and C25 CF_3 groups display typical CF_3 rotational disorder. One of the six unique tfac ligands, that of O11,12 attached to Mn3, is positionally disordered with 65 : 35 ratio for the occupancies of CH_3 at C29 and CF_3 at C30 *versus* the reverse. No noticeable distortions in the remaining interatomic distances and angles in the β-diketonate could be detected from this positional disorder. Only two previous structures with the tfac ligand are reported in the literature, Mn(tfac)$_2$(TMED), CSD refcode: DEVPAY,[1] and Mn(tfac)$_3$, XOYBEV,[40] in both of which the tfac ligands are positionally ordered.

The mononuclear complex in the structure of **4** is found in a general position, but despite this, displays a rotational disorder of one of the two tfac methyl groups, that of C4, which was constrained using AFIX 127 with refined occupancy ratios of 62 : 38. In a structure of comparable quality, the complex in **5** is also in a general position, but shows residual rotational disorders (minor components of 14–30% occupancies) in three of the four CF_3 groups.

By contrast, the structure found for the complex in **6** has low lattice displacements, and combined displacement/rotational disorder was detected in a single CF_3 group, that of C4. H-bonding involves both aqua ligand hydrogens as donors and

two of the four hfac O atoms as acceptors. Parameters for this are available in Section 7, Table S48 of the SI. A persistent, large residual peak in the final difference map occurs at 2.23 Å from Mn and could be attributed to a case of whole molecule disorder. In view of the smallness of the second component, only the Mn atom of the second component was considered, using a two-part disorder model, which refined to <10% occupancy. For further information, see Section 7 of the SI.

The monomeric complex in **7** crystallizes on a mirror plane that contains the Mn ion and the oxygen atoms of the THF ligand. Consequently, the two hfac ligands are mirror images of each other, with an ordered C4 CF_3 and a rotationally disordered C5 CF_3. Each are mirror imaged. The puckered THF ligands therefore also are reflection disordered and show rather larger displacement ellipsoids.

Similarly, the monomeric complex in structure **8** lies on a mirror plane containing the Mn ion, the aqua ligand O and the whole of the $NCCH_3$ ligand. The structure is ordered, except that the C7 methyl group H atoms are reflection disordered across the plane of symmetry. Both aqua ligand H atoms donate to two of the four hfac O atoms to form infinite H-bonded chains of molecules in the [100] direction. Parameters can be found in Section 9, Table S65 of the SI.

Conclusions

The promising properties of Mn_xO_y and Mn_xF_y thin films and nanostructured materials provide an impetus to seek a deeper understanding of reactants and reaction conditions that will grant control over nanomaterial design and functionality. Of the numerous preparatory methods and starting materials currently employed, deposition and thermal decomposition of manganese complexes of β-diketonates offer a unique opportunity for customizability, compatible with low-cost CVD or ALD methodologies.[1,2,26,31] Despite significant interest, structural studies and synthetic reports of manganese β-diketonates remain relatively limited. In pursuit of anhydrous Mn(II) complexes of fluorinated β-diketonates, tfac and hfac, we have encountered surprising structural diversity. Using comparable synthetic strategies, we have observed important differences in product, depending on whether tfac or hfac is employed. While $Mn(hfac)_2(OH_2)_2$ is readily prepared and isolated *via* multiple synthetic procedures reported here and elsewhere,[21,26] $Mn(tfac)_2(OH_2)_2$ was previously unknown and indeed our attempts to prepare this species resulted in the identification of three novel structures: a coordination polymer, $\{K[Mn(tfac)_3]\}_\infty$ **1**; the water solvate of the target aqua species, $Mn(tfac)_2(OH_2)_2 \cdot H_2O$ **2**; and a unique trinuclear species, $Mn_3(tfac)_6(OH_2)_2$ **3**. For both tfac and hfac, displacement of aqua ligands with *O*,*O*′-bidentate DME occurred reproducibly and reliably to generate the $Mn(tfac)_2$(DME) **4** and $Mn(hfac)_2$(DME) **5** complexes, respectively. It is possible to displace one of the two aqua ligands of $Mn(hfac)_2(OH_2)_2$ with THF, generating $Mn(hfac)_2(OH_2)$(THF) **6**. Displacement of both aqua ligands of $Mn(hfac)_2(OH_2)_2$ with THF to generate anhydrous $Mn(hfac)_2(THF)_2$ **7** is facile so long as an adequate drying agent is employed. Interestingly, we have also isolated $Mn(hfac)_2(OH_2)$(THF) **6** from inadvertently introducing trace amounts of water into a reaction mixture containing anhydrous $Mn(hfac)_2(THF)_2$ **7**. Moreover, trace acetonitrile was also inadvertently introduced, and $Mn(hfac)_2(OH_2)(NCCH_3)$ **8** was isolated as well. The results of careful observation and analysis of products from both successful and failed reactions provide a snapshot of the interesting landscape of Mn(II) β-diketonate structures. On the one hand, serving as a cautionary tale, these results also suggest a much wider diversity of accessible structures and stoichiometries, encouraging further exploration and creativity in this fascinating field.

Author contributions

Conceptualization, funding acquisition, supervision, and writing – original draft, KEP; formal analysis, data curation, RTB; investigation and writing – review and editing, MAI and RTB.

Conflicts of interest

There are no conflicts to declare.

Data availability

CCDC 2441294–2441298 and 2441638–2441640 (**1** to **8**) contain the supplementary crystallographic data for this paper.[41a–h]

Supplementary information: Crystallographic tables and detailed structural information files. See DOI: **https://doi.org/10.1039/d5ra03587b**.

Acknowledgements

The authors thank M. D'Agostino at Brock University for Elemental Analysis measurements and Dr Alan Lough at the University of Toronto for single crystal XRD data measurement and structure solution of **4** and **7**. This study was supported by funding from the Natural Sciences and Engineering Research Council (NSERC) of Canada Discovery Grant (DG; grant no. RGPIN-2020-03969) program (KEP), NSERC Canada Graduate Scholarship – Doctoral (NSERC CGS – D) program (MAI), the University of Guelph College of Engineering and Physical Sciences (CEPS) Dean's Tri-Council Scholarship (MAI). RTB gratefully acknowledges career support from the NSERC. The diffractometer at the University of Lethbridge X-ray Diffraction Facility was purchased by the University and the Faculty of Arts & Science.

References

1 C. Maccato, L. Bigiani, G. Carraro, A. Gasparotto, R. Seraglia, J. Kim, A. Devi, G. Tabacchi, E. Fois, G. Pace, V. Di Noto and D. Barreca, *Chem.–Eur. J.*, 2017, **23**, 17954–17963.
2 D. Barreca, G. Carraro, E. Fois, A. Gasparotto, F. Gri, R. Seraglia, M. Wilken, A. Venzo, A. Devi, G. Tabacchi and C. Maccato, *J. Phys. Chem. C*, 2018, **122**, 1367–1375.

3 S. Zhu, S.-H. Ho, C. Jin, X. Duan and S. Wang, *Environ. Sci.: Nano*, 2020, **7**, 368–396.
4 C. E. Frey and P. Kurz, *Chem.–Eur. J.*, 2015, **21**, 14958–14968.
5 Z. Chen, Z. Jiao, D. Pan, Z. Li, M. Wu, C. H. Shek, C. M. Wu and J. K. Lai, *Chem. Rev.*, 2012, **112**, 3833–3855.
6 K. Wang, X. Ma, Z. Zhang, M. Zheng, Z. Geng and Z. Wang, *Chem.–Eur. J.*, 2013, **19**, 7084–7089.
7 Z. Y. Fei, B. Sun, L. Zhao, W. J. Ji and C. T. Au, *Chem.–Eur. J.*, 2013, **19**, 6480–6487.
8 D. M. Robinson, Y. B. Go, M. Mui, G. Gardner, Z. Zhang, D. Mastrogiovanni, E. Garfunkel, J. Li, M. Greenblatt and G. C. Dismukes, *J. Am. Chem. Soc.*, 2013, **135**, 3494–3501.
9 Z. Bai, B. Sun, N. Fan, Z. Ju, M. Li, L. Xu and Y. Qian, *Chem.–Eur. J.*, 2012, **18**, 5319–5324.
10 L. Zhang, Q. Zhou, Z. Liu, X. Hou, Y. Li and Y. Lv, *Chem. Mater.*, 2009, **21**, 5066–5071.
11 Y. Li, H. Tan, X. Y. Yang, B. Goris, J. Verbeeck, S. Bals, P. Colson, R. Cloots, G. Van Tendeloo and B. L. Su, *Small*, 2011, **7**, 475–483.
12 B. H. Xiao, K. Xiao, J. X. Li, C. F. Xiao, S. Cao and Z. Q. Liu, *Chem. Sci.*, 2024, **15**, 11229–11266.
13 W. Gong, B. Fugetsu, Z. Wang, I. Sakata, L. Su, X. Zhang, H. Ogata, M. Li, C. Wang, J. Li, J. Ortiz-Medina, M. Terrones and M. Endo, *Commun. Chem.*, 2018, **1**, 1–8.
14 H. Zhang, B. Li and E. V. Dikarev, *J. Cluster Sci.*, 2008, **19**, 311–321.
15 J. Britten, N. G. R. Hearns, K. E. Preuss, J. F. Richardson and S. Bin-Salamon, *Inorg. Chem.*, 2007, **46**, 3934–3945.
16 R. A. Mayo, I. S. Morgan, D. V. Soldatov, R. Clérac and K. E. Preuss, *Inorg. Chem.*, 2021, **60**, 11338–11346.
17 E. M. Fatila, J. Goodreid, R. Clérac, M. Jennings, J. Assoud and K. E. Preuss, *Chem. Commun.*, 2010, **46**, 6569–6571.
18 D. J. Sullivan, R. Clérac, M. Jennings, A. J. Lough and K. E. Preuss, *Chem. Commun.*, 2012, **48**, 10963–10965.
19 E. M. Fatila, R. Clérac, M. Rouzières, D. V. Soldatov, M. Jennings and K. E. Preuss, *J. Am. Chem. Soc.*, 2013, **135**, 13298–13301.
20 J. Liang and J. W. Canary, *Angew. Chem.*, 2010, **122**, 7876–7879.
21 M. L. Morris, R. W. Moshier and R. E. Sievers, *Inorg. Chem.*, 1963, **2**, 411–412.
22 S. L. Lehotay, A. R. Lightfield, J. A. Harman-Fetcho and D. J. Donoghue, *J. Agric. Food Chem.*, 2001, **49**, 4589–4596.
23 F. J. Schenck, P. Callery, P. M. Gannett and J. R. Daft, *J. AOAC Int.*, 2002, **85**, 1177–1180.
24 H. B. Gray and C. H. Langford, *C&EN*, 1968, 68–76.
25 C. H. Langford and H. B. Gray, *Ligand Substitution Processes*, W. A. Benjamin, Inc., New York, 1965.
26 S. I. Troyanov, O. Y. Gorbenko and A. A. Bosak, *Polyhedron*, 1999, **18**, 3505–3509.
27 Z. Wei, A. S. Filatov and E. V. Dikarev, *J. Am. Chem. Soc.*, 2013, **135**, 12216–12219.
28 O. V. Kuznetsova, E. Y. Fursova, G. A. Letyagin, G. V. Romanenko and V. I. Ovcharenko, *Russ. Chem. Bull., Int. Ed.*, 2018, **67**, 1202–1205.
29 E. Y. Fursova, O. V. Kuznetsova, V. I. Ovcharenko, G. V. Romanenko and A. S. Bogomyakov, *Russ. Chem. Bull., Int. Ed.*, 2008, **57**, 1198–1205.
30 A. Escuer, J. Esteban, J. Mayans and M. Font-Bardia, *Eur. J. Inorg. Chem.*, 2014, 5443–5450.
31 N. Pienack, P. Lindenberg, G. Doungmo, N. Heidenreich, F. Bertram, M. Etter, M. T. Wharmby and H. Terraschke, *Z. Anorg. Allg. Chem.*, 2018, **644**, 1902–1907.
32 H. H. Loffler, A. M. Mohammed, Y. Inada and S. Funahashi, *J. Comput. Chem.*, 2006, **27**, 1944–1949.
33 R. Åkesson, L. G. M. Pettersson, M. Sandström and U. Wahlgren, *J. Am. Chem. Soc.*, 1994, **116**, 8705–8713.
34 J. R. Bryant, J. E. Taves and J. M. Mayer, *Inorg. Chem.*, 2002, **41**, 2769–2776.
35 M. H. Dickman, *Acta Crystallogr.*, 1997, **53**, 402–404.
36 H. Adams, N. A. Bailey, D. E. Fenton and R. A Khalil, *Inorg. Chim. Acta*, 1993, **209**, 55–60.
37 Y.-L. Gao, K. Y. Maryunina, S. Hatano, S. Nishihara, K. Inoue and M. Kurmoo, *Cryst. Growth Des.*, 2017, **17**, 4893–4899.
38 M. A. Palacios, A. Rodríguez-Diéguez, A. Sironi, J. M. Herrera, A. J. Mota, V. Morena, J. Cano and E. Colacio, *New J. Chem.*, 2009, **33**, 1901–1908.
39 M. G. F. Vaz, H. Akpinar, G. P. Guedes, S. Santos Jr, M. A. Novak and P. M. Lahti, *New J. Chem.*, 2013, **37**, 1927–1932.
40 R. Gostynski, P. H. van Rooyen and J. Conradie, *J. Mol. Struct.*, 2020, **1201**, 127119.
41 (*a*) M. A. Ibrahim, R. T. Boeré and K. E. Preuss, CCDC 2441294: Experimental Crystal Structure Determination, 2025, DOI: **10.5517/ccdc.csd.cc2mycfd**; (*b*) M. A. Ibrahim, R. T. Boeré and K. E. Preuss, CCDC 2441295: Experimental Crystal Structure Determination, 2025, DOI: **10.5517/ccdc.csd.cc2mycgf**; (*c*) M. A. Ibrahim, R. T. Boeré and K. E. Preuss, CCDC 2441296: Experimental Crystal Structure Determination, 2025, DOI: **10.5517/ccdc.csd.cc2mychg**; (*d*) M. A. Ibrahim, R. T. Boeré and K. E. Preuss, CCDC 2441297: Experimental Crystal Structure Determination, 2025, DOI: **10.5517/ccdc.csd.cc2mycjh**; (*e*) M. A. Ibrahim, R. T. Boeré and K. E. Preuss, CCDC 2441298: Experimental Crystal Structure Determination, 2025, DOI: **10.5517/ccdc.csd.cc2myckj**; (*f*) M. A. Ibrahim, R. T. Boeré and K. E. Preuss, CCDC 2441638: Experimental Crystal Structure Determination, 2025, DOI: **10.5517/ccdc.csd.cc2myqjv**; (*g*) M. A. Ibrahim, R. T. Boeré and K. E. Preuss, CCDC 2441639: Experimental Crystal Structure Determination, 2025, DOI: **10.5517/ccdc.csd.cc2myqkw**; (*h*) M. A. Ibrahim, R. T. Boeré and K. E. Preuss, CCDC 2441640: Experimental Crystal Structure Determination, 2025, DOI: **10.5517/ccdc.csd.cc2myqlx**.